arXiv:astro-ph/0509207v2 9 Sep 2005

Total masses of the Local Group and M 81 group derived from the local Hubble flow

I.D.Karachentsev[1] **and O.G.Kashibadze**[2]

[1]Special Astrophysical Observatory, Russian Academy of Sciences, N.Arkhyz, KChR, 369167, Russia
[2] Moscow State University, Moscow, Russia

Abstract

Based on accurate measurements of distances to nearby galaxies made with Hubble Space Telescope, we determined the radii of the zero-velocity surface: $R_0 = 0.96 \pm 0.03$ Mpc for the Local Group and $R_0 = 0.89 \pm 0.05$ Mpc for the group of galaxies around M 81/M 82. This yields the total masses of the groups to be $M_T = (1.29 \pm 0.14)10^{12} M_\odot$ and $M_T = (1.03 \pm 0.17)10^{12} M_\odot$, respectively. The R_0–method allowed us to determine the mass ratio of the brightest two members in the considered groups. Based on the minimum scatter of galaxies with respect to the Hubble regression, we derived a mass ratio of 0.8 : 1.0 for the Milky Way and Andromeda, and 0.54 : 1.00 for M 82 and M 81, which is quite close to the ratio of luminosities of these galaxies.

1 Introduction.

Until recently the use of the virial relation $2T + U = 0$ between the kinetic (T) and potential (U) energy of a group of galaxies was the only method of calculating the mass of a system of galaxies on scales of (0.1 - 1.0) Mpc. However, the uncertainty in membership of some galaxies even in very nearby groups, the possible absence of a supposed virial equilibrium and also the unknown character of predominating motions in groups make virial estimates of the mass not quite reliable tool, especially in the case of loose groups.

As has been noted by Lynden-Bell (1981), any group as a large concentration of mass, has a decelerating effect on the surrounding Hubble flow. At small distances from the center of a group, the "velocity - distance" relation departs from the linear Hubble law $V = H_0 R$ and crosses the zero-velocity line at a value of $R = R_0$ which was named "the radius of the zero-velocity surface". According to Lynden-Bell, in the case of spherical symmetry the total mass of the group M_T and the radius R_0 are related by a simple equation

$$M_T = (\pi^2/8G) \times R_0^3 \times T_0^{-2}, \quad (1)$$

where G is the gravity constant and T_0 is the age of the universe. Thus, the determination of the value of R_0 from observational data enables the mass of the group to be computed since the third parameter in (1), the age of the universe, is now known with a sufficiently high accuracy, $T_0 = 13.7 \pm 0.2$ Gyr (Spergel et al. 2003). These considerations were used by Sandage (1986, 1987) and Giraud (1990) to estimate the mass of the Local Group. Based on distances and radial velocities of a dozen of nearby galaxies, Sandage (1986) calculated the total mass of the Local Group (LG) to be $4 \times 10^{11} M_\odot$. At that time, the

distances to even the nearest galaxies were measured with low accuracy. For instance, Sandage adopted the following distances: 1.58 Mpc for Leo A (best present value 0.69 Mpc), 1.66 Mpc for NGC 300 (best present value 2.15 Mpc), 2.51 Mpc for Pegasus dIr (0.76 Mpc), 2.63 Mpc for NGC 2403 (3.30 Mpc), 5.75 Mpc for M 81 (3.63 Mpc), and 6.31 Mpc for IC 342 (3.28 Mpc). Here we show in brackets the present-day distances of these galaxies derived from luminosities of cepheids or the tip of the red giant branch. Recently, Karachentsev et al. (2002a) have used accurate estimates of distances and radial velocities for the most nearby 38 galaxies in the neighborhood of the LG and obtained a value of the total mass of the group to be $(1.3\pm0.3)10^{12}M_{\odot}$, i.e. three times as high as the Sandage's estimate. This approach was applied later by Karachentsev et al.(2002b) to the determination of R_0 and M_T for other nearby groups around M 81, Centaurus A, IC 342, NGC 253 (Sculptor filament), and NGC 4736 (Canes Venatici cloud). The summary of the estimates of the total masses of the groups and their comparison with the virial mass estimates were presented by Karachentsev (2005). As the comparison showed, in the groups of galaxies with a "crosing time" $T_{cross} < (2H_0)^{-1}$ the mass estimates from internal (virial) motions and from external Hubble pattern of velocities are in agreement within the measurement errors (∼30-40%). It is evident, however, that the new method deriving the total mass for a group from R_0 needs to be discussed in more detail.

2 Observational data and determination of R_0.

Consider a group of galaxies with the center at "C" (Figure 1a), which is located from us (LG) at a distance D_c and is receding along the line of sight at a velocity V_c. Let there be a galaxy G in the vicinity of the group at a distance D_g from the observer, which is moving along the line of sight at a velocity V_g. At an angular separation Θ between C and G, their mutual linear distance R is

$$R^2 = D_g^2 + D_c^2 - 2D_g \times D_c \times cos\Theta, \tag{2}$$

and the mutual velocity difference in projection onto the line between them is

$$V_{gc} = V_g \times \cos\lambda - V_c \times \cos\mu, \tag{3}$$

where $\mu = \lambda + \Theta$,

$$tang\lambda = D_c \times \sin\Theta/(D_g - D_c \times \cos\Theta) \tag{4}$$

Here we assumed that random peculiar velocities of the galaxies are low as compared with the velocities of the regular Hubble flow.

For plotting the relationship between V_{gc} and R we made use of the data on radial velocities and distances of galaxies in the neighborhood of the Milky Way, Andromeda (M 31) and M 81. The basic source of data was the Catalog of Neighboring Galaxies = CNG (Karachentsev et al. 2004) complemented by the latest measurements of distances to nearby galaxies. The data used below are collected in Table 1 whose columns contain: (1,2) galaxy number and name; (3,4) its Galactic coordinates; (5,6) heliocentric radial velocity and its standard measurement error; (7) radial velocity reduced to the centroid of the LG with the apex parameters from NED (NASA Extragalactic Database); (8,9)

measured distance to galaxy and its error (in Mpc); (10) so-called tidal index or index of galaxy isolation

$$TI_i = \max[\log(M_k/D_{ik}^3] + C, \quad k = 1, 2, ... \tag{5}$$

where M_k is the mass of a neighboring galaxy located at a distance D_{ik} from the one considered; a constant C is choosen so that the negative values of TI correspond to isolated galaxies of the general field, while the positive values to group members; (11) reference to a source of data on the galaxy distance. We included into this sample only the galaxies with accurate measurements of distances, most of the distances were determined from the tip of the red giant branch (TRGB) with a typical error of ∼10%. Some preliminary distance estimates made in the current surveys of nearby galaxies, which are carried out with ACS at Hubble Space Telescope for the programs of Karachentsev (# 9971, #10235) and Tully (#10210) are designated as Kar05, Kar06 and Tully05, respectively. Our sample contains a total of 133 nearby galaxies. About 35 another galaxies are also known in this volume, but their distances have so far been measured with low accuracy or else radial velocity measurements are absent.

Using the velocities and distances from columns (5,6) of Table 1, we constructed a Hubble diagram V_{LG} vs. D_{MW} for the nearest 104 galaxies in a sphere of radius 4 Mpc from us. The members of groups with $TI > 0$ are shown on this diagram (Fig. 2) by open circles, while the isolated galaxies with $TI < 0$ are presented by filled circles. The horizontal and vertical bars at them indicate standard errors of the distance and velocity. The solid line in the figure corresponds to a Hubble regression with a parameter $H_0 = 72$ km s^{-1} Mpc^{-1} bent at small distances because of the gravitation deceleration by the mass of the Local Group. From the family of regressions with the same value of H_0 and different values of M_{LG} (or R_0) only one regression is shown for which the sum of squares of deviations of galaxies is a minimum. This regression crosses the zero-velocity line at $R_0 = 0.73$ Mpc.

As can be seen from this diagram, the dispersion of velocities of galaxies relative to the Hubble regression rises markedly at $R = 3$ - 4 Mpc. This is due to galaxies in groups around M 81 and IC 342/Maffei with high virial motions. Two of them (KDG 63 and KDG 61) have velocities close to zero with respect to the LG centroid. Provided that the Hubble diagram is continued to distances $\sim 15 - 20$ Mpc, we again find there galaxies with velocities $V_{LG} < 0$, which are located in the zone of high virial motions in the Virgo cluster. To elucidate the role played virial motions, we have drawn in Fig. 2 another regression line using the field galaxies only. In the figure it is displaied by a dotted line, and gives a somewhat smaller value, $R_0 = 0.69$ Mpc.

3 The radius R_0 and the LG centroid position.

As it is known, the Local Group has a binary dumbell-like shape. The Milky Way with its companions and Andromeda (M 31) with its companions are separated by a distance of 0.77 Mpc and approaching one another at a velocity of 123 km s^{-1}. We consider below to what extent the estimate of the zero velocity radius for the LG depends on the position of its center of mass. We suppose that the center of mass of our group is on the line connecting the Milky Way and Andromeda at an arbitrary relative distance $x = D_c/D_{M31}$. For each value of x with a step of 0.05 in the range from 0 (the center

resides in the Milky Way) to 1 (the center coincides with M 31) the galaxy distances and velocities were calculated, using expressions (2) and (3). In each case we constructed a Hubble diagram similar to that shown in Fig.2 and determined the radius R_0 by a χ^2 – criterion. The results are presented in Table 2. Column 1 indicates the relative position of the center of mass, the second and third columns present the value of the radius R_0 for all galaxies and separately for isolated galaxies. The fourth column displays the dispersion of velocities relative to the Hubble regression, and the last one shows the velocity dispersion after quadratic subtraction of errors, $H_0\sigma_D$, caused by the errors of distances. To diminish the contribution of virial motions in the LG and nearby groups, we computed R_0, σ_v and σ_{vc} in the interval of distances from 0.6 to 2.6 Mpc with respect to the LG centroid. The data presented in Table 2 allow us to draw the following conclusions:

a) The radius of the zero-velocity surface changes in a limited interval from 0.73 to 0.97 Mpc (0.69 – 1.02 Mpc for the field galaxies) at any position of the center of masses of the LG between the Milky Way and Andromeda, which is evidence of robust estimation of R_0 on the basis of the observational data available.

b) At different positions of the LG center of masses, the dispersion of velocities of the galaxies with respect to the Hubble regression varies from 23 to 61 km s^{-1}, and with allowance made for distance measurement errors σ_{vc} varies in the range (13 – 46) km s^{-1}. For this reason, the Hubble flow around the LG is rather cold.

c) Adopting a minimum value of σ_v or σ_{vc} as an indicator of an optimum position of the LG center of mass, we obtain the value of $x = D_c/D_{M31} = 0.55 \pm 0.05$. This means that the masses of our Galaxy and M 31 are related as $M_{MW} : M_{M31} = 0.80 : 1.00$. This is in good agreement with the ratio of their maximum rotation velocities V_m. According to Fukugita & Peebles (2004), $V_m(MW) = 241 \pm 13$ km s^{-1}, while LEDA (Lyon Extragalactic Database) gives V_m (M 31) $= 259 \pm 5$ km s^{-1}. Since the masses (luminosities) of spiral galaxies are approximately proportional to the cubic power of V_m, then the ratio of masses following from the presented data is $M_{MW} : M_{M31} = 0.8 : 1.0$, right the same as our estimate.

The Hubble diagram for the vicinities of the LG with the position of the centroid at a distance $D_c = 0.55 \times D_{M31} = 0.42$ Mpc is presented in Fig. 3. The upper panel of the figure exhibits the distribution of the galaxies in velocities and distances relative to the center of masses with indication of errors in measured velocities and distances. The lower panel contains the original numbers of all the galaxies in Table 1. As one can see from the figure, the position of the radius of the zero-velocity surface is the most sensitive to the velocities and distances of only a few "strategically situated" galaxies: Leo A, WLM, DDO 210, and Sag DIR.

4 R_0 and tangential motions

We have supposed so far tangential velocities of galaxies to be negligibly small. In order to check the degree this assumption affects the estimate of the radius R_0, we have performed numerical simulations of the Hubble diagram, adding the tangential component to the radial velocity of each galaxy from Table 1. The distribution of tangential velocities was assumed to be Gaussian with a mean $< V_t >$ and a standard deviation $\sigma(V_t) = 30$ km s^{-1}. The orientation of the tangential velocity vector in positional angle was assigned to be

uniformly random. Assuming different positions of the LG centroid, we performed a lot of Monte-Carlo simulations at $< V_t > = 35$ km s^{-1} and $< V_t >= 70$ km s^{-1}. The latter value corresponds to the dispersion of radial velocities in the LG and M 81 group. The results of determination of the radius R_0 for 10 series of simulations at $D_c = 0.55 D_{M31}$ are listed in Table 3. As it follows from these data, the estimates of the radius fluctuate about the mean value $R_0 = 0.96$ Mpc with a characteristic scatter of 0.03 Mpc.

Returning to the estimate of the LG total mass, we adopt in (1) the age of the universe to be $T_0 = 13.7 \pm 0.2$ Gyr (Spergel et al. 2003), which leads to an expression

$$M_T/M_\odot = 1.46 \times 10^{12} \times (R_0/Mpc)^3. \quad (6)$$

With the indicated error in the estimate of T_0 and the value of the radius of the zero-velocity surface $R_0 = (0.96 \pm 0.03)$ Mpc, the total mass of the Local Group is $M_T(LG) = (1.29 \pm 0.14) 10^{12} M_\odot$. Disregarding the mass of other members of the LG, we obtain the values of the total mass of the two main members of the group: $M_{MW} = 5.8 \times 10^{11} M_\odot$ and $M_{M31} = 7.1 \times 10^{11} M_\odot$.

5 The radius R_0 for M 81 group

The Hubble diagram for galaxies in the neighborhood of M 81 is presented in Fig. 4. All the designations here are the same as in Fig. 2. Velocities and distances are expressed with reference to the group centroid coincided with the brightest member, M 81. The crossing of the Hubble regression with the zero-velocity line gives $R_0 = 1.10$ Mpc. The regression only for isolated galaxies (dotted curve) results in a somewhat smaller value, $R_0 = 1.05$ Mpc.

As it is known, a galaxy, second in luminosity in this group, is M 82 whose radial velocity is by 240 km s−1 higher than in M 81. Considering that the center of masses of the group lies on the line connecting M 81 and M 82, we determined the velocities and distances of galaxies with respect to a new center and constructed appropriate Hubble regressions. The results are tabulated in Table 4. Its first column indicates the relative position of the center between M 81 ($x = 0$) and M 82 ($x = 1$), the second and the third columns give values of the radius R_0 derived for all galaxies and for the field galaxies only, the last two columns contain values of the dispersion of velocities with or without taking account of errors in distances of galaxies, $H_0\sigma_D$. Estimates of R_0 and σ_v were made only over the galaxies situated within $R = 0.6$ - 3.0 Mpc from the group center. Two inferences can be made from the presented data:

a) The dispersion of velocities of galaxies relative to the Hubble regression reaches a minimum at the position of the center of masses at a distance of $x = 0.35 \pm 0.05$ from M 81 toward M 82. A mass ratio of the two galaxies, $M_{M82} : M_{M81} = (0.54 \pm 0.12) : 1.00$, corresponds to this value. The derived mass ratio is consistent, within the errors, with the ratio of infrared K-luminosities of these galaxies, $L_{M82} : L_{M81} = 0.47 : 1.00$, from the data of the 2MASS survey.

b) The same as in the case of the LG neighborhood, the galaxies around the M 81 group demonstrate that the Hubble flow is surprisingly "cold". The dispersion of velocities relative to the Hubble regression at an optimum position ($x = 0.35$) of the center of masses

of the group is no higher than 30 km s^{-1}, and with allowance made for measurements errors it drops a few km s^{-1}.

The Hubble diagram for galaxies around M 81 and M 82 at $x = 0.35$ is exhibited in Fig. 5. Its upper panel shows errors of the measured distances and velocities of the galaxies. In the lower panel we indicate the galaxy numbers labeled by in Table 1. For the determination of the radius R_0 the most crucial are the positions of the galaxies UGC 6456 = VII Zw 403, NGC 4236, KKH 37 and UGC 7242, which makes them attractive targets for application of more refined methods of distance estimation.

To define the role of possible tangential motions, we undertook numerical simulations of the Hubble flow around M 81/M 82 given the same parameters as in the case of the LG. At a mean tangential velocity of the galaxies $< V_t > = 35$ km s^{-1}, we obtained actually the same position of the center of mass, $< x >= 0.35 \pm 0.03$ and the mean value of the radius $< R_0 >= 0.89 \pm 0.05$ Mpc. The simulations made with $< V_t >= 70$ km s^{-1} left these parameters almost unchanged but increased their errors: $< x >= 0.37 \pm 0.05$ and $< R_0 >= 0.87 \pm 0.10$ Mpc. Adopting for R_0 the value of 0.89 ± 0.05 Mpc, we obtain an estimate of the total mass of the group $M_T = (1.03 \pm 0.17)10^{12} M_\odot$. Then, neglecting the contribution of other members of the group, we derive individual masses $M_{M81} = 6.7 \times 10^{11} M_\odot$ and $M_{M82} = 3.6 \times 10^{11} M_\odot$ for the brightest two galaxies.

6 Another application of the R_0- method.

P.J.E.Peebles (2005) directed our attention to the existence of another approach to estimating the radius of the zero-velocity surface for a group or cluster. Let a galaxy G falls radially on the center of a group C at a velocity V_i (see Fig.1b). If the center of the group is moving away from us at a velocity V_c directed along the line of sight, then the velocity along the line of sight of the galaxy G which is located at an angular separation Θ from the group center will be

$$V_g = V_c \times \cos\Theta - V_i \times \cos\lambda. \tag{7}$$

The falling velocity of the galaxy is then expressed as

$$V_i = [V_c \times \cos\Theta - V_g]/\cos\lambda, \tag{8}$$

and it is precisely this velocity should be compared with the distance of the galaxy from the group center found from (2) when describing the pattern of motions of galaxies around a massive group. When the angles λ and Θ are small (i.e. the galaxy is located strictly in front or behind the group center), equations (3) and (8) yield an about the same infall velocity toward the group center. Apparently, at angles λ close to 90° the discrepancy between the two approaches becomes significant.

In order to determine the radius R_0 by the new method, we plotted a Hubble diagram for the Local Group and its neighborhood at the position of the center of masses on $x = D_c/D_{M31} = 0.55$. Using expression (8) and excluding galaxies with $\cos\lambda < 0.7$, we obtained a value $R_0 = 0.92$ Mpc (and 0.78 Mpc for field galaxies with $TI < 0$). The dispersion of velocities relative to the Hubble regression proven to be equal to 29 km s^{-1}, or 18 km s^{-1} after taking account of errors in galaxy distances. As one can see, in the case

of the LG the differences in the estimates of R_0 and σ_v for the two approaches turn out to be small. However, exploring the Hubble flow around the M 81 group by this method, we found considerable discrepancies. At the former of the center of masses, $x = 0.35$, and with the exclusion of galaxies having $\cos\lambda < 0.7$, we obtained a significantly larger radius $R_0 = 1.31$ Mpc (or 1.23 Mpc for the field galaxies). The scatter of galaxies on the Hubble diagram also increased, making $\sigma_v = 70$ km s^{-1} and $\sigma_{vc} = 35$ km s^{-1}

A direct comparison of the two discussed methods of estimating the radius R_0 is now impeded because of absence of observational data on tangential velocities of galaxies. However, such data may be available in the near future after completion of cosmic projects like SIM (Space Interferometric Mission) described by Peebles et al. (2001). In the absence of data on space vectors of galaxy velocities these two methods lay actually different emphasis on the properties of the Hubble flow in the vicinity of nearby groups. In the former case we supposed that most of the galaxies under study are not in the "infall zone" but on the asimptotic Hubble relationship (the model of the minor attractor). The latter approach assumes that numerous galaxies being discussed are involved in the infall zone (the model of the major extended attractor). The Hubble diagrams in Fig.3 and 5 sugest the former approach to be preferred.

7 Concluding remarks

The measurements of distances of many nearby galaxies accomplished during the last 2–3 years to an accuracy of ∼10% served us an observational basis for determination of the masses of nearby groups not from internal (virial) motions, but from the external Hubble field of velocities around the groups. The application of this method put forward by Lynden-Bell (1981) and Sandage (1986) assume the following conditions to be satisfied: 1) spherically symmetric shape of the group potential well, 2) small random motions of galaxies relative the regular Hubble flow, and 3) sufficiently high number density of test particles (galaxies) for which radial velocities and distances are known with high accuracy.

Based on the most recent measurements of distances to galaxies made with Hubble Space Telescope, we determined the radii of the zero-velocity surface: $R_0 = 0.96 \pm 0.03$ Mpc for the LG and $R_0 = 0.89 \pm 0.05$ Mpc for the group of galaxies around M 81/M 82. With the errors indicated, the formal accuracy of estimation of the total mass of the groups by the new method is only ∼15%, which is by about a factor three better than from virial motions. However, the R_0–method is probably to contain systematic errors which need a special study.

At integrated luminosities $L_B = 10.1 \times 10^{10} L_\odot$ for the LG and $L_B = 6.1 \times 10^{10} L_\odot$ for the M 81 group (Karachentsev, 2005), their total mass-to-blue luminosity ratios make only $(12.8 \pm 1.4) M_\odot/L_\odot$ and $(16.9 \pm 2.8) M_\odot/L_\odot$, respectively. The obtained values of M_T/L_B are much lower than the old virial estimates $M_T/L_B \sim 100 M_\odot/L_\odot$ (Tully, 1987), which were considered to be typical of poor groups of galaxies. Since more than half of galaxies in the Local volume are members of such groups, this results in a rather low average density of matter in the Local volume.

Random motions of galaxies relative to the regular Hubble flow makes only 15 - 25 km s^{-1} within $(1-3)R_0$ around the LG and 3– 28 km s^{-1} in a similar zone around M 81. The observed "coldness" of the local Hubble flow is independent evidence of low density

of the part of matter in the Local volume which concentrates in groups.

It is also interest that the R_0–method made it possible to determine the mass ratio in the brightest two members of the discussed groups. Based on the minimum scatter of galaxies with respect to the Hubble regression, we derived a mass ratio of 0.8 : 1.0 for the Milky Way and Andromeda, and found a ratio of masses of 0.54 : 1.00 for M 82 and M 81, which is quite close to the ratio of luminosities of these galaxies.

It is pleasure to thank P.J.E. Peebles for very useful discussions. We used in this work the NASA Extragalactic Database (NED), Lyon Extragalactic Database (LEDA) and the data of the 2 Micron All Sky Survey (2MASS). The work was supported through grant of RFBR 04–02–16115 and grant DFG–RFBR 02–02–04012.

References

[1] Cannon J.M., Skillman E.D., Sembach K.R., Bomans D.J., 2005, ApJ, 618, 247

[2] Fingerhut R.L., McCall M.L., De Robertis M., et al. 2003, ApJ 587, 672

[3] Fukugita M., P.J.E. Peebles, 2004, ApJ 616, 643

[4] Giraud E., 1990, A&A 231, 1

[5] Karachentsev, I.D., Dolphin, A.E., et al. 2002b, A&A 383, 125

[6] Karachentsev, I.D., Makarov, I.D., et al. 2002a, A&A 389, 812

[7] Karachentsev, I.D., Karachentseva V.E., Huchtmeier W.K., Makarov, I.D., 2004, AJ 127, 2031 (= CNG)

[8] Karachentsev, I.D., 2005, AJ 129, 178

[9] Lynden-Bell, D., 1981, Observatory 101, 111

[10] Peebles P.J.E., 2005, personal communication

[11] Peebles P.J.E., Phelps S.D., Shaya E.J., Tully R.B., 2001, ApJ 554, 104

[12] Sandage, A. 1986, ApJ 307, 1

[13] Sandage, A. 1987, ApJ 317, 557

[14] Seth A.C., Dalkanton J.J., de Jong R.S., 2005, AJ 129, 1331

[15] Silva D.R., Massey P., DeGioia-Eastwood K., Henning P.A., 2005, ApJ 623, 148

[16] Spergel D.N. et al. 2003, ApJS 148, 175

[17] Tully R.B., 1987, ApJ 321, 280

Table 1: Galaxies with accurate distances and radial velocities in/around the Local Group and the M81 group.

N	Name	l	b	V_h	$\pm dV$	V_{LG}	D_{MW}	$\pm dD$	TI	Reference
		deg	deg	km/s		km/s	Mpc			
1	WLM	75.86	−73.62	−116	2	−10	0.92	0.04	0.3	CNG
2	ESO349-31	351.48	−78.12	207	7	216	3.21	0.31	0.5	Kar05
3	NGC55	332.67	−75.74	129	3	111	2.12	0.21	−0.4	Seth et al.05
4	IC10	118.97	−3.34	−344	1	−60	0.66	0.06	1.8	CNG
5	ESO294-10	320.42	−74.42	117	5	81	1.92	0.19	1.0	CNG
6	NGC147	119.82	−14.25	−193	3	85	0.76	0.08	3.0	CNG
7	AndIII	119.37	−26.26	−355	9	−92	0.76	0.07	3.5	CNG
8	NGC185	120.79	−14.48	−202	3	73	0.62	0.06	2.3	CNG
9	NGC205	120.72	−21.14	−244	3	24	0.83	0.11	3.7	CNG
10	NGC221	121.15	−21.98	−145	6	121	0.77	0.04	6.8	CNG
11	M31	121.17	−21.57	−301	1	−35	0.77	0.04	4.6	CNG
12	AndI	121.68	−24.82	−380	11	−120	0.81	0.03	3.7	CNG
13	NGC247	113.94	−83.56	160	2	215	3.65	0.38	1.3	Kar05
14	NGC253	97.43	−87.97	241	2	274	3.94	0.37	0.3	CNG
15	DDO6	119.39	−83.88	295	5	348	3.34	0.24	0.5	CNG
16	SMC	302.81	−44.33	158	4	−22	0.06	0.01	3.5	CNG
17	NGC300	299.21	−79.42	144	5	114	2.15	0.10	−0.3	CNG
18	Sculptor	287.53	−83.16	110	1	96	0.09	0.01	2.8	CNG
19	LGS-3	126.77	−40.88	−286	5	−74	0.62	0.02	1.7	CNG
20	IC1613	129.79	−60.56	−232	1	−89	0.73	0.02	0.9	CNG
21	KKH5	125.49	−11.35	39	2	304	4.26	0.43	−1.2	CNG
22	NGC404	127.03	−27.01	−48	9	195	3.06	0.37	−1.0	CNG
23	AndV	126.22	−15.12	−403	4	−143	0.81	0.04	2.8	CNG
24	AndII	128.92	−29.16	−188	3	46	0.68	0.02	2.4	CNG
25	M33	133.61	−31.33	−180	3	36	0.85	0.04	2.0	CNG
26	KKH6	129.68	−10.21	17	1	270	3.73	0.38	−0.8	Kar05
27	NGC625	273.67	−73.12	405	1	335	3.89	0.39	−0.4	Cannon et al.05
28	Phoenix	272.16	−68.95	−13	29	−106	0.44	0.02	0.8	CNG
29	Maffei1	135.86	−0.55	66	22	297	3.01	0.60	2.7	Fingerhut et.04
30	Fornax	237.29	−65.65	53	9	−32	0.14	0.01	2.3	CNG
31	KK35	138.20	10.30	105	1	320	3.16	0.32	2.4	CNG
32	IC342	138.17	10.58	31	3	245	3.28	0.27	−0.1	CNG
33	UGCA86	139.77	10.64	67	4	275	2.96	0.31	0.3	Kar05
34	CamA	137.25	16.20	−47	1	164	3.93	0.47	0.1	CNG
35	UGCA92	144.70	10.51	−99	5	89	3.01	0.31	1.1	Kar05
36	NGC1560	138.37	16.02	−36	5	171	3.45	0.36	1.0	CNG
37	CamB	143.38	14.42	77	5	266	3.34	0.32	1.0	CNG
38	UGCA105	148.52	13.66	111	5	279	3.15	0.32	0.3	CNG
39	LMC	280.47	−32.89	278	2	28	0.05	0.01	3.6	CNG

N	Name	l	b	V_h	$\pm dV$	V_{LG}	D_{MW}	$\pm dD$	TI	Reference
		deg	deg	km/s		km/s	Mpc			
40	KKH34	140.42	22.35	110	1	299	4.61	0.46	−0.8	CNG
41	Carina	260.11	−22.22	223	60	−53	0.10	0.01	2.7	CNG
42	KKH37	133.98	26.54	10	1	214	3.39	0.33	−0.3	Kar05
43	HIZSS003	217.71	0.09	280	1	101	1.69	0.17	−0.6	Silva et al.05
44	NGC2366	146.43	28.53	99	3	253	3.19	0.41	1.0	CNG
45	NGC2403	150.57	29.19	131	3	268	3.30	0.36	0.0	CNG
46	HoII	144.28	32.69	157	1	311	3.39	0.20	0.6	CNG
47	KDG52	143.82	33.01	113	5	268	3.55	0.26	0.7	CNG
48	DDO53	149.30	34.95	20	1	151	3.56	0.24	0.7	CNG
49	UGC4483	144.97	34.38	156	1	304	3.21	0.18	0.5	CNG
50	HoI	140.73	38.65	139	1	291	3.84	0.46	1.5	CNG
51	NGC2976	143.92	40.90	3	5	139	3.56	0.38	2.7	CNG
52	BK3n	142.31	40.83	−40	5	101	4.02	0.26	1.0	CNG
53	M81	142.09	40.90	−35	4	107	3.63	0.34	2.2	CNG
54	M82	141.40	40.57	202	4	347	3.53	0.26	2.7	CNG
55	KDG61	142.50	41.28	−116	30	23	3.60	0.25	3.9	CNG
56	A0952+69	141.74	40.92	100	5	243	3.87	0.21	1.9	CNG
57	LeoA	196.90	52.42	24	4	−40	0.69	0.06	0.2	CNG
58	SexB	233.20	43.78	301	1	111	1.36	0.07	−0.7	CNG
59	NGC3109	262.10	23.07	403	1	110	1.33	0.08	−0.1	CNG
60	NGC3077	141.90	41.66	13	4	153	3.82	0.38	1.9	CNG
61	Antlia	263.10	22.31	362	1	66	1.32	0.06	2.3	CNG
62	KDG63	144.13	43.10	−129	5	0	3.50	0.24	1.8	CNG
63	LeoI	225.98	49.11	285	2	128	0.25	0.02	1.5	CNG
64	SexA	246.15	39.88	324	1	94	1.32	0.04	−0.6	CNG
65	SexdSph	243.50	42.27	226	2	8	0.09	0.01	2.8	CNG
66	HS117	138.14	41.30	−37	5	116	3.96	0.39	1.9	Kar05
67	DDO78	141.14	44.00	55	9	191	3.72	0.26	1.8	CNG
68	IC2574	140.20	43.60	57	2	197	4.02	0.41	0.9	CNG
69	DDO82	137.90	42.18	56	3	207	4.00	0.40	0.9	CNG
70	KDG73	136.88	44.23	116	6	263	3.70	0.22	1.3	CNG
71	LeoII	220.16	67.23	76	5	−18	0.21	0.02	1.7	CNG
72	UGC6456	127.84	37.33	−103	1	89	4.34	0.43	−0.3	CNG
73	UGC6541	151.90	63.27	250	4	304	3.89	0.47	−0.7	CNG
74	NGC3738	144.56	59.32	228	4	305	4.90	0.49	−1.0	CNG
75	NGC3741	157.57	66.45	230	4	264	3.03	0.30	−0.8	CNG
76	KK109	156.85	68.98	212	1	241	4.51	0.45	−0.6	CNG
77	DDO99	166.20	72.75	242	1	248	2.64	0.21	−0.5	CNG
78	NGC4068	138.91	63.04	210	3	290	4.31	0.42	−1.0	Kar05
79	NGC4163	163.21	77.70	163	5	164	2.96	0.29	0.1	Kar05
80	ESO321-14	294.85	24.05	613	5	337	3.19	0.26	−0.3	CNG

N	Name	l	b	V_h	$\pm dV$	V_{LG}	D_{MW}	$\pm dD$	TI	Reference
		deg	deg	km/s		km/s	Mpc			
81	UGC7242	128.87	50.60	68	2	213	5.42	0.52	0.4	Kar05
82	KDG90	161.10	78.06	280	6	283	2.86	0.14	1.6	CNG
83	NGC4214	160.26	78.07	291	3	295	2.94	0.18	−0.7	CNG
84	UGC7298	135.22	64.06	173	1	255	4.21	0.42	−0.7	CNG
85	NGC4236	127.41	47.36	0	4	160	4.45	0.44	−0.4	CNG
86	NGC4244	154.56	77.16	243	1	255	4.49	0.45	0.0	CNG
87	IC3104	301.41	−16.95	430	5	171	2.27	0.19	−0.5	CNG
88	NGC4395	162.08	81.54	320	1	315	4.61	0.46	0.1	CNG
89	DDO126	148.60	78.74	218	5	231	4.87	0.49	0.1	CNG
90	DDO125	137.75	72.94	195	4	240	2.54	0.17	−0.9	CNG
91	NGC4449	136.85	72.40	201	4	249	4.21	0.42	0.0	CNG
92	UGC7605	150.99	80.13	310	1	317	4.43	0.44	0.7	CNG
93	NGC4605	125.33	55.47	143	5	276	5.47	0.53	−1.1	Kar05
94	IC3687	131.95	78.46	358	1	385	4.57	0.46	1.1	CNG
95	NGC4736	123.36	76.01	309	1	353	4.66	0.47	−0.5	CNG
96	GR8	310.74	76.98	214	3	136	2.10	0.34	−1.2	CNG
97	IC4182	107.71	79.09	320	1	356	4.70	0.65	0.6	CNG
98	DDO165	120.75	49.36	31	1	196	4.57	0.46	0.0	CNG
99	UGC8215	114.58	70.03	218	1	297	4.55	0.45	−0.5	Kar05
100	DDO167	111.62	70.32	163	6	243	4.19	0.47	0.0	CNG
101	DDO168	110.76	70.66	194	1	273	4.33	0.43	0.0	CNG
102	NGC5102	309.73	25.84	467	7	230	3.40	0.39	0.7	CNG
103	NGC5204	113.50	58.01	203	1	341	4.65	0.46	−1.1	CNG
104	UGC8508	111.14	61.31	62	5	186	2.56	0.15	−1.0	CNG
105	NGC5237	311.88	19.22	361	4	122	3.33	0.33	2.1	Kar05
106	UGC8638	23.28	78.99	274	1	273	4.27	0.40	−1.3	Kar05
107	DDO181	89.73	73.12	202	1	272	3.02	0.31	−1.3	Tully05
108	ESO325-11	313.51	19.91	540	4	307	3.40	0.39	1.1	CNG
109	DDO183	77.79	73.45	191	1	257	3.18	0.32	−0.8	Tully05
110	KKH86	339.04	62.60	287	3	209	2.61	0.16	−1.5	CNG
111	UGC8833	69.71	73.96	226	5	285	3.12	0.31	−1.4	Tully05
112	KK230	63.71	71.99	62	2	126	1.92	0.18	−1.0	Kar05
113	DDO187	25.57	70.46	152	4	172	2.28	0.22	−1.3	Tully05
114	DDO190	82.01	64.48	150	4	263	2.79	0.26	−1.3	CNG
115	UMin	104.95	44.80	−247	1	−44	0.06	0.01	3.3	CNG
116	ESO274-01	326.80	9.33	522	5	335	3.12	0.30	−1.0	Kar06
117	KKR25	83.88	44.41	−139	2	68	1.86	0.12	−0.7	CNG
118	Draco	86.36	34.75	−293	21	−48	0.08	0.01	3.0	CNG
119	MilkyWay	0.73	0.57	0	10	−88	0.01	0.00	2.5	CNG
120	IC4662	328.55	−17.85	308	4	145	2.44	0.24	−0.9	Kar05
121	NGC6503	100.57	30.64	43	7	301	5.27	0.53	−1.2	CNG

N	Name	l	b	V_h	$\pm dV$	V_{LG}	D_{MW}	$\pm dD$	TI	Reference
		deg	deg	km/s		km/s	Mpc			
122	SagdSph	5.61	−14.09	142	4	161	0.02	0.00	5.6	CNG
123	NGC6789	94.97	21.52	−141	9	144	3.60	0.36	−1.4	CNG
124	SagDIG	21.06	−16.28	−77	4	23	1.04	0.07	−0.3	CNG
125	NGC6822	25.34	−18.40	−57	2	64	0.50	0.01	0.6	CNG
126	DDO210	34.05	−31.34	−137	5	13	0.94	0.04	−0.1	CNG
127	IC5152	343.92	−50.19	124	3	75	2.07	0.18	−1.1	CNG
128	UGCA438	11.86	−70.86	62	5	99	2.23	0.15	−0.7	CNG
129	CasdSph	109.46	−9.96	−307	2	−5	0.79	0.04	2.0	CNG
130	Pegasus	94.77	−43.55	−184	2	60	0.76	0.08	1.2	CNG
131	KKH98	109.09	−22.38	−137	3	151	2.45	0.13	−0.7	CNG
132	PegdSph	106.04	−36.32	−354	3	−94	0.82	0.02	1.7	CNG
133	NGC7793	4.52	−77.17	229	2	252	3.91	0.41	0.1	CNG

Table 2: The Hubble flow parameters for the Local Group.

Centroid position	R_0	R_0,field	σ_v	σ_{vc}
	Mpc	Mpc	km/s	km/s
0.00	0.73	0.69	31.9	20.5
0.05	0.76	0.70	31.4	19.8
0.10	0.77	0.71	30.6	19.0
0.15	0.78	0.73	29.9	18.3
0.20	0.79	0.74	29.4	17.8
0.25	0.79	0.75	29.1	17.2
0.30	0.81	0.77	28.9	17.0
0.35	0.83	0.79	28.6	16.8
0.40	0.83	0.80	28.3	16.7
0.45	0.85	0.81	28.1	16.6
0.50	0.86	0.83	27.8	16.3
0.55	0.95	0.89	23.8	12.8
0.60	0.90	0.89	37.7	22.4
0.65	0.92	0.91	38.5	23.2
0.70	0.93	0.92	39.6	24.3
0.75	0.94	0.94	40.5	25.2
0.80	0.96	0.96	41.7	26.4
0.85	0.97	0.97	42.8	27.5
0.90	0.97	0.99	50.3	34.3
0.95	0.81	1.01	59.7	44.0
1.00	0.88	1.02	61.0	46.3

Table 3: The radius R_0 for the Local Group for x = 0.55 and tangential motions.

R_0 (Mpc) (V_t = 35 km/s)	R_0 (Mpc) (V_t = 70 km/s)
0.99	0.89
0.96	1.03
0.95	0.96
0.96	0.98
0.95	0.91
0.94	0.95
0.99	1.02
0.96	0.97
0.91	0.98
0.95	0.95
Mean 0.96±0.02	0.96±0.04

Table 4: The Hubble flow parameters around M81 group.

Centroid position	R_0 (Mpc)	R_0,field (Mpc)	σ_v (km/s)	σ_{vc} (km/s)
0.00	1.10	1.05	49.9	22.2
0.05	1.07	1.03	45.4	17.7
0.10	1.04	1.01	41.2	13.5
0.15	1.01	0.98	37.2	9.7
0.20	0.98	0.96	33.7	6.2
0.25	0.95	0.94	31.0	3.4
0.30	0.92	0.92	29.1	1.5
0.35	0.89	0.90	28.2	0.6
0.40	0.83	0.86	30.1	2.5
0.50	0.80	0.84	32.6	5.0
0.55	0.79	0.82	35.7	8.2
0.60	0.77	0.80	39.4	11.8
0.65	0.74	0.78	43.6	16.1
0.70	0.71	0.76	48.2	20.6
0.75	0.69	0.74	53.0	25.5
0.80	0.66	0.72	58.0	30.5
0.85	0.63	0.70	63.0	35.5
0.90	0.60	0.69	68.4	40.8
0.95	0.63	0.67	73.8	46.3
1.00	0.60	0.65	79.4	51.9

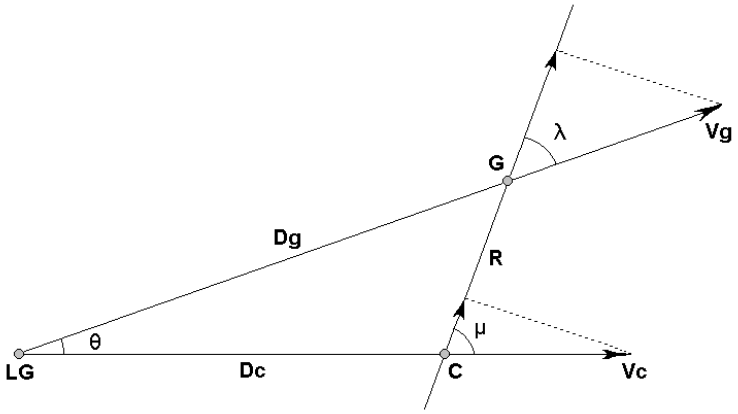

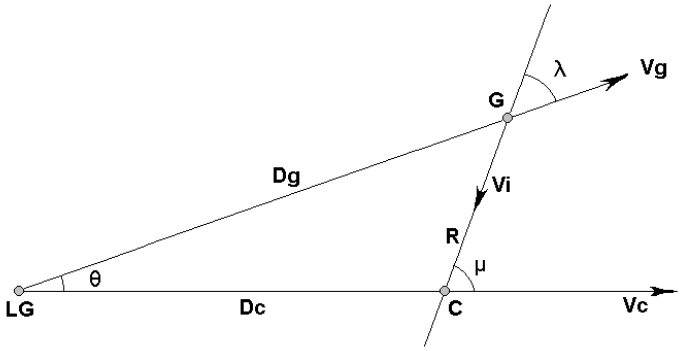

Figure 1: Diagrams of motion of a galaxy relative to group center.

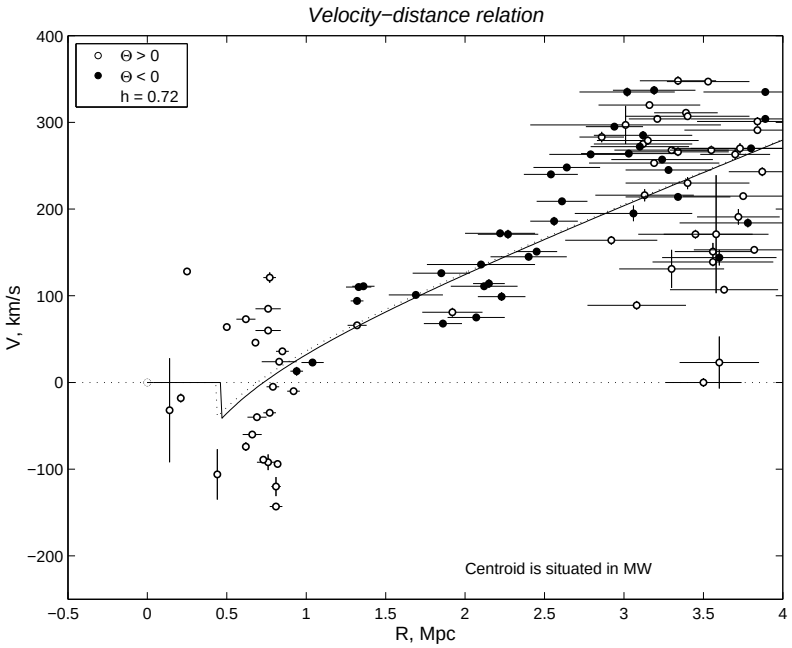

Figure 2: Hubble diagram for the Local Group with the center in the Milky Way.

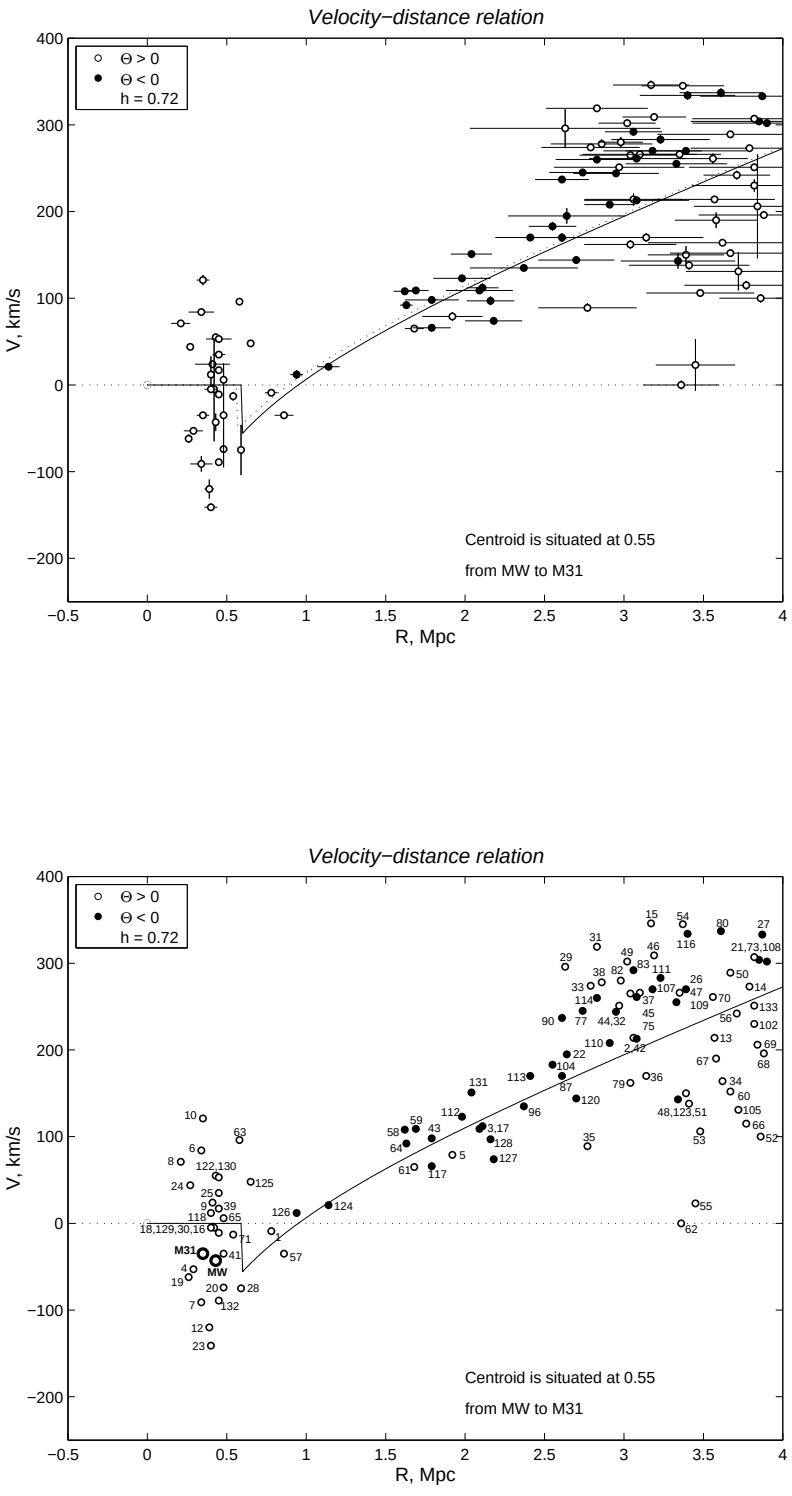

Figure 3: Hubble diagram for the Local Group with the center of masses at $x = 0.55$ towards M 31.

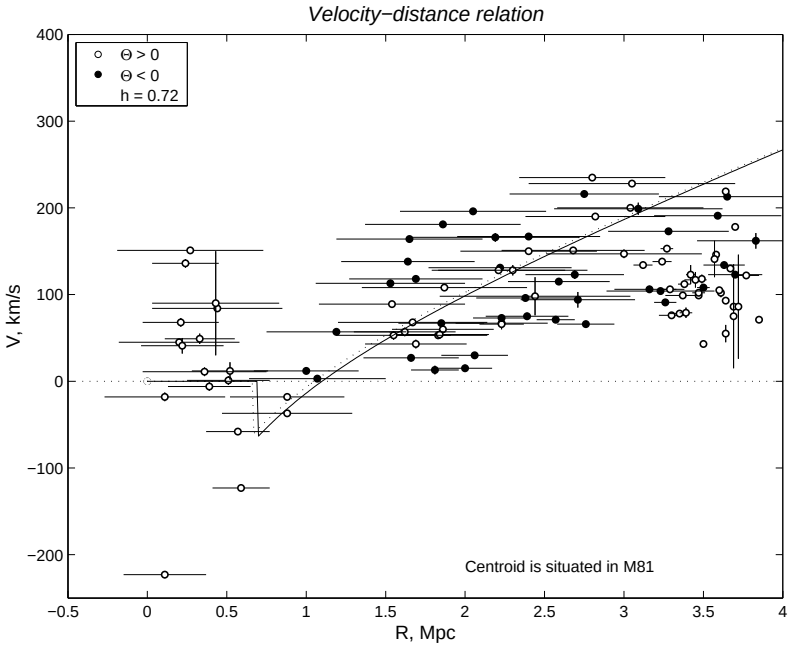

Figure 4: Hubble diagram for the M 81 group with the center in M 81

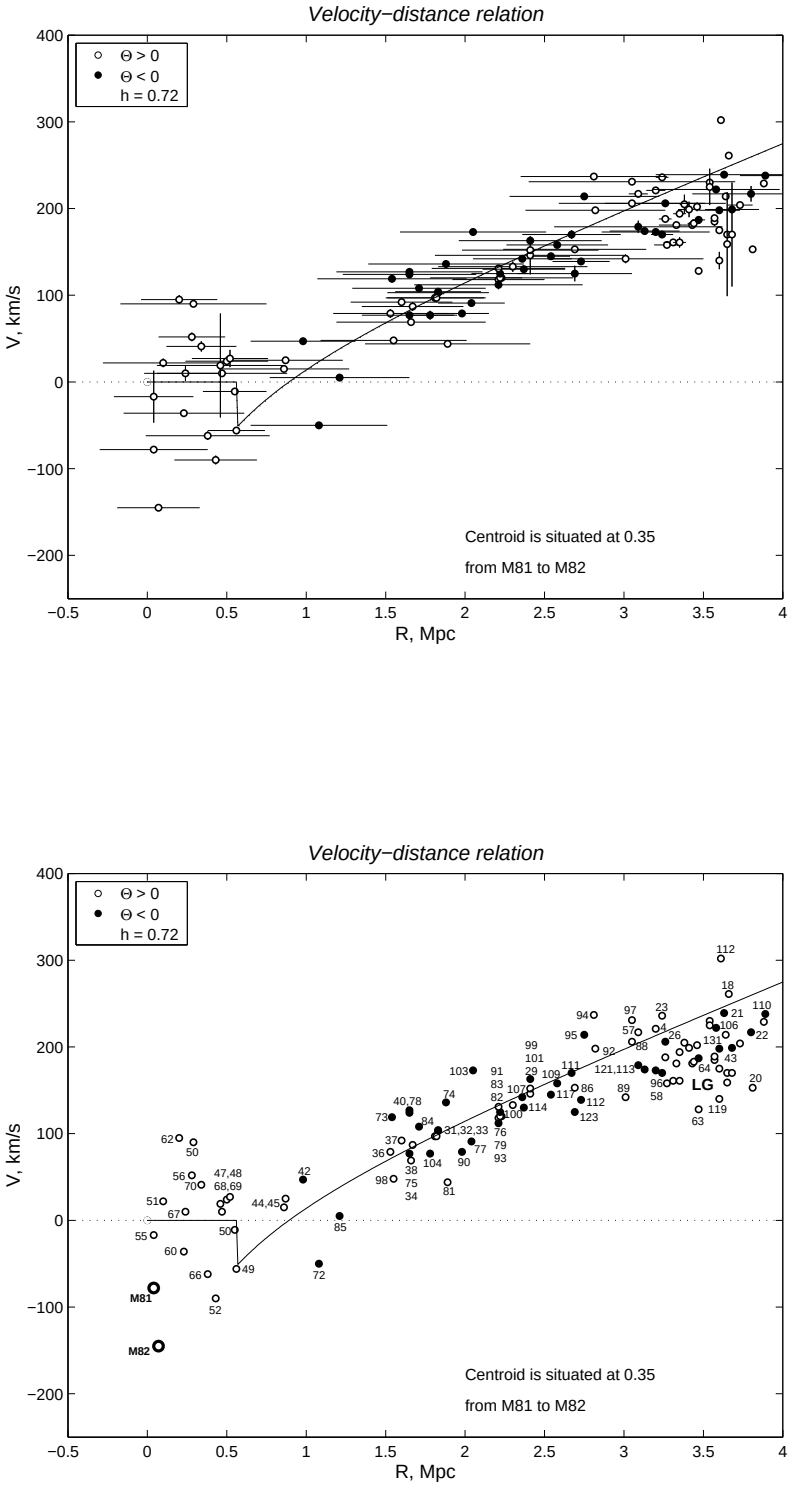

Figure 5: Hubble diagram for the M 81 group with the center of masses at $x = 0.35$ towards M 82.